HHS Public Access

Author manuscript

*Nature*. Author manuscript; available in PMC 2010 April 14.

Published in final edited form as:

*Nature*. 2009 January 1; 457(7225): 57–62. doi:10.1038/nature07668.

# WSTF regulates the function of H2A.X via a novel tyrosine kinase activity

**Andrew Xiao**[1], **Haitao Li**[2], **David Shechter**[1], **Sung Hee Ahn**[1], **Laura A. Fabrizio**[3], **Hediye Erdjument-Bromage**[3], **Satoko Ishibe-Murakami**[2], **Bin Wang**[4], **Paul Tempst**[3], **Kay Hofmann**[5], **Dinshaw J. Patel**[2], **Stephen J. Elledge**[4], and **C. David Allis**[1,*]

[1]Laboratory of Chromatin Biology, The Rockefeller University, New York, NY

[2]Structural Biology Program, Memorial-Sloan-Kettering Cancer Center, New York, NY

[3]Molecular Biology Program, Memorial-Sloan-Kettering Cancer Center, New York, NY

[4]Howard Hughes Medical Institute, Department of Genetics, Harvard Partners Center for Genetics and Genomics, Harvard Medical School, Boston, MA

[5]Miltenyi Biotec GmbH, Koeln, Germany

## Summary

DNA double-stranded breaks present a serious challenge for eukaryotic cells. Inability to repair breaks leads to genomic instability, carcinogenesis, and cell death. During the DSB response, mammalian chromatin undergoes reorganization demarcated by H2A.X Ser139 phosphorylation (γ-H2A.X). However, the regulation of γ-H2A.X phosphorylation and its precise role in chromatin remodeling during the repair process remain unclear. Here, we report a novel regulatory mechanism mediated by WSTF, a component of the WICH ATP-dependent chromatin remodeling complex. We show that WSTF has intrinsic tyrosine kinase activity via a domain that shares no sequence homology to any known kinase fold. We show that WSTF phosphorylates Tyr142 of H2A.X and that WSTF activity plays an important role in regulating a number of events that are critical for the DNA damage response. Our work reveals a novel mechanism that regulates the DNA damage response and expands our knowledge of domains that contain intrinsic tyrosine kinase activity.



*Correspondence and requests for materials should be addressed to C.D.A (alliscd@rockefeller.edu).

**Author Information** Reprints and permissions information is available at npg.nature.com/reprints and permissions. The authors do not have any competing financial interests. Correspondence and requests for materials should be addressed to alliscd@rockefeller.edu.

Supplemental information is linked to the online version of the paper at XXX. A detailed discussion of the function of WSTF and H2A.X Y142 phosphorylation is also included as SI.

**Author contributions** A.X. designed the study, performed the experiments and wrote the paper; H. Li generated recombinant WSTF protein and performed CD analysis; D.S. helped with the experiments performed in *Xenopus* egg extracts and edited the manuscript; S. H. A. generated and analyzed *H2A L132Y* mutant yeast strain; L. A. F., H. E. B. and P.T. performed MS analysis; S. I. B. provided technical assistance for protein production; B.W. and S. J. E. provided MDC1 constructs; K. H. did bioinformatical analysis on the WSTF kinase domain; D.J. P. provided general guidance for generating recombinant WSTF. S. J. E. also discussed results and commented on the manuscript. C. D. A. provided support and general guidance for this work.

One hallmark of the mammalian DNA double-strand break (DSB) response is the formation of Ionizing Radiation Induced Foci (IRIF), which are composed of compacted chromatin and numerous DNA repair and checkpoint proteins[1,2]. Despite considerable progress in understanding signaling pathways leading to checkpoint control and DNA repair, the nature of the specialized chromatin structures at IRIF is not well understood. One of the earliest events occurring at IRIF is the phosphorylation of H2A.X, a specialized histone H2A variant, at S139 (referred to as γ-H2A.X) by the ATM and ATR kinases[3]. H2A.X-deficient mouse embryonic fibroblasts (MEFs) and B and T cells display pronounced levels of genomic instability[4]. Class switch recombination and spermatogenesis are also defective in H2A.X deficient mice, further implying its involvement in DNA damage repair[4-6]. Moreover, H2A.X-deficiency accelerates B and T cell lymphoma development in p53-deficient mice[5,7]. Consistent with these functions in mammalian cells, phosphorylation of the equivalent site on yeast H2A (S129) is found at DSB sites and spreads to ∼50Kb of the flanking regions[8]. In mammals, this phosphorylation event directly recruits Mdc1 and sets in motion the recruitment of additional factors such as 53BP1, RNF8, and the Brca1 A complex[9]. Furthermore, several recent studies have also indicated that ATP-dependent chromatin remodeling complexes are engaged in DNA repair pathways at these sites. The yeast NuA4 and INO80 complexes, for example, are recruited to the damaged chromatin via γ-H2A.X[10,11,12].

Mammalian H2A.X bears significant differences with lower eukaryotes. For example, H2A.X is a minor H2A variant in mammalian cells (1-10%[3]) while the major yeast form of H2A is most similar to H2A.X because it contains the signature C-terminal sequence of mammalian H2A.X[3]. In mammalian cells, the loss of SWI/SNF chromatin remodeling complex expression leads to defects in the H2A.X DNA damage response. However, it is unclear whether these defects are due to the lack of direct regulation by the SWI/SNF complex or other indirect pathways[13]. Given the unique features of mammalian H2A.X, we sought to find new factors that are directly involved in regulating H2A.X. Our results define a novel DNA damage response pathway regulating H2A.X function, mediated through the WSTF-SNF2H chromatin remodeling complex and the phosphorylation of H2A.X at Tyr142 in mammals. Unexpectedly, we determined that the amino-terminal domain of WSTF, including its WAC domain, exhibits tyrosine kinase activity towards Tyr142 of H2A.X. We further show that the novel tyrosine kinase activity of WSTF is required for eliciting a number of critical molecular events during the DNA damage response in mammalian cells.

## Regulation of Y142 Phosphorylation

A role in the DNA damage response for mammalian H2A.X (γ-H2A.X) is well documented, although its regulation and underlying mechanism of action is only partially understood (reviewed in [ref 3]). Further inspection of the C-terminus of H2A.X revealed a tyrosine (Tyr142 in mammals) that exists in metazoans, but is absent in unicellular eukaryotes such as yeast (Figure 1a). Interestingly, two forms of H2A.X exist in the *Xenopus* genome, which are different at this residue (the “F” and “Y” form, Figure 1a), are differentially expressed during development (D.S., A.X., C.D.A, et al, in press). Although recent studies suggest a role for Y142 in recruiting Mdc1[14,15,16,17-19] the *in vivo* function of Y142, especially in the regulation of γ-H2A.X, remains unclear[17]. We hypothesized that Y142 might be

phosphorylated in H2A.X under certain physiological conditions (Figure 1b). Preliminary studies using a pan anti-phosphotyrosine antibody indicated that H2A.X was phosphorylated prior to DNA damage (data not shown). To investigate further whether Tyr142 is indeed phosphorylated, an antibody raised against an extreme C-terminal peptide containing phosphorylated Y142 of H2A.X was generated and shown to be highly selective for H2A.X Y142 phosphorylation (hereafter, α-H2A.X Y142ph; Supplementary Figure S1). In MEF cells, Tyr142 is constitutively phosphorylated under normal growth conditions and becomes gradually dephosphorylated during the DNA damage response, while γ-H2A.X increases (Figure 1b). As it has been reported that H2A.X is highly enriched in *Xenopus* oocytes and eggs[20],[21], we asked whether its Y142 phosphorylation status would be altered in response to DNA damage treatment, in the context of *Xenopus* early embryonic development. Similar to mammalian cells, Y142 phosphorylation levels are significantly decreased in response to DNA damage (Supplementary Figure S1a).

Since the major form of H2A in yeast carries the "SQEL" motif (Figure 1a and[3]), we examined whether a point mutant mimicking the mammalian "SQEY" motif would constitute a new phospho-acceptor. Similar to the mammalian cells, this mutant yeast strain (L132Y) is strongly reactive to α-H2A.X Y142ph antibodies with reactivity greatly diminished following DNA damage treatment (Supplementary Figure S1b). Collectively, these results raise the intriguing possibility that an evolutionarily conserved DNA damage regulated phosphotyrosine pathway exists and regulates H2A.X and likely other DNA damage responsive proteins.

## The WSTF-SNF2H complex interacts with H2A.X

To investigate novel mechanisms that regulate H2A.X function, we sought to isolate protein complexes directly associated with H2A.X *in vivo*. Primary H2A.X-/- MEF cells were reconstituted with H2A.X constructs (WT or Y142F mutant), with or without an N-terminal FLAG epitope tag. The FLAG tag did not interfere with typical DNA damage response pathways, including γ-H2A.X (data not shown). Three independent cell lines (WT and mutants) were constructed in which the expression levels were comparable (50-80%) to the control primary MEFs (with two intact endogenous H2A.X alleles) and the majority of the reconstituted cells (~90%) have similar expression levels (data not shown). To enrich for proteins or complexes that may associate with H2A.X mononucleosomes, we adapted an approach that successfully enriched such chromatin particles for subsequent biochemical purifications[22]. This method, followed by immunoprecipitation with α-FLAG antibodies, significantly enriched H2A.X containing mononucleosomes and associated proteins (Figure 2a and Supplementary Figure S2). As shown by silver staining, a small number of polypeptides besides histones were associated with the wild type H2A.X mononucleosomes at a stoichiometric level, the amount of which was decreased after cells were treated with ionizing radiation (Figure 2b). In addition, these interactions are reduced with Y142F mutant H2A.X mononucleosomes (Figure 2b). Subsequent mass spectrometry (MS) analysis demonstrated that two of the more prominent proteins are SNF2H (140 KDa), a mammalian homolog of the ISWI ATPase[23],[24], and WSTF [William-Beuren syndrome Transcription Factor (171 KDa), a.k.a. BAZ1B, a member of the BAZ/WAL family chromatin remodeling factors (Supplementary Figure S3)[25],[26],[27]. These proteins constitute the WICH complex

(WSTF-ISWI ATP-dependent chromatin–remodeling complex), which mobilizes nucleosomes *in vitro* and is suggested to be involved in the regulation of DNA replication[28],[29].

We also investigated if other protein factors present in ISWI-containing chromatin remodeling complexes, such as CHRAC15 and 17[30], co-purified with H2A.X-containing mononucleosomes at sub-stoichiometric levels. However, none of these components were detected by either MS or immunoblotting approaches (data not shown), leading us to the tentative conclusion that only the WICH complex copurifies with H2A.X-containing mononucleosomes at significant levels *in vivo*. We next confirmed this association results by immunoblot analyses of the complexes co-immunoprecipitated with H2A.X-containing nucleosomes. Consistent with the MS results, WSTF and SNF2H were enriched in these complexes (Figure 2c).

To investigate the roles of WSTF in regulating the function of H2A.X, several independent WSTF knock-down NIH3T3 cell lines (WSTF RNAi cells) were generated by infection with a short hairpin WSTF RNAi construct, in which WSTF protein expression is significantly reduced (Figure 2d). Additionally, we attempted to knockdown SNF2H with a similar approach, but SNF2H knockdown resulted in S-phase defects and cell death (data not shown) as described in SNF2H knock-out mice studies[31]; presumably, SNF2H functions in additional chromatin remodeling complexes that are involved in a variety of vital cell functions[24]. The specificity of the RNAi knock-down approach was demonstrated by rescuing WSTF expression with the human WSTF gene (the sequences in the WSTF mRNA targeted by the RNAi construct are different between human and mouse) (see below and Figure 4). Most interestingly, WSTF deficiency leads to a decrease in Y142 phosphorylation (Figure 2d), indicating that WSTF may be also directly involved in regulating Y142 phosphorylation *in vivo* (see below). These data suggest a novel regulatory mechanism of H2A.X that involves the WICH complex and Tyr142 phosphorylation.

## WSTF is a novel tyrosine kinase that phosphorylates Y142 of H2A.X

To further investigate the function of WSTF, we purified recombinant, full-length human WSTF proteins in insect cells (Figure 3a). A single protein band migrating at the expected molecular weight (171 KDa) was detected with silver staining (Figure 3b). MS analysis on the purified samples confirmed that this protein was WSTF and did not detect any other proteins except trace amounts of heat shock proteins (data not shown). The recombinant full length WSTF protein phosphorylated H2A.X-containing nucleosomes (Figure 3b) that were reconstituted *in vitro*, using ATP and divalent manganese ion $Mn^{2+}$ (but not $Mg^{2+}$, see Supplementary Figure S4) as cofactors. To address whether WSTF can specifically phosphorylate Y142 of H2A.X, we also reconstituted Y142F mutant nucleosomes. The Y142F mutant does not impact histone octamer or nucleosome formation during reconstitution (data not shown). In *in vitro* kinase assays, WSTF phosphorylated the WT but not Y142F H2A.X, indicating that Y142 is the major site of phosphorylation (Figure 3b). The *in vitro* kinase activity of WSTF towards Y142 of H2A.X was confirmed by immunoblotting using α-H2A.X Y142ph antibodies (Figure 3c).

Since no detectable proteins other than trace amounts of heat shock proteins co-purified with WSTF from insect cells (Figure 3b), we hypothesized that WSTF has an intrinsic kinase activity. However, WSTF does not share homology with known kinase domains. Therefore we generated truncated recombinant WSTF proteins (Figure 3a) to investigate which portion of the protein is required for this novel kinase activity. Using this approach, we demonstrated the N-terminal portion of WSTF is necessary and sufficient for kinase activity, strongly indicating that the kinase motif resides in its N-terminal portion (Figure 3d). Additional structure function analyses determined that residues 1-345 contained the active kinase domain composed of a WAC domain and a newly identified C-motif that are both required for optimal kinase activity (Figure 3e & g and **Methods**). A C388A mutation generated a kinase dead allele that maintained proper folding (Figure 3f, Supplementary Figure S6 and **Methods**). To further confirm the intrinsic activity of the putative WSTF kinase domain, we generated recombinant WSTF proteins in *E. coli*, since protein kinases, especially tyrosine kinases, are rare in the *E. coli* genome. Bioinformatic and biochemical analysis of the kinase domain of WSTF reveals two well-structured motifs (N-motif, containing the conserved WAC domain[27] and a previously unreported C-motif, Figure 3a and Supplementary Figure S7). Co-expression of both motifs restores the kinase activity, while the N-terminal motif alone had a much reduced activity (Figure 3g). These results strongly indicate that the N- and C- motif are required for the optimal kinase activity. Collectively, our results demonstrate that WSTF has a previously unidentified intrinsic kinase activity via a novel kinase domain.

## WSTF plays a critical role in foci formation

As the functions of the WICH complex, especially that of WSTF, in the DNA damage response have not been explored, we investigated the role of WSTF in the DNA damage response. Upon DNA damage treatment, the initial γ-H2A.X phosphorylation of H2A.X and its foci formation in WSTF RNAi cells (as described in Figure 2) were similar to control cells (up to 1-hour post IR, Figure 4a). However, in control cells, the γ-H2A.X level remained unchanged until 16-hour post IR. In contrast, the level of γ-H2A.X phosphorylation rapidly declined in WSTF RNAi cells 4 hours after IR treatment (Figures 4a). It is well-established that the number and morphology of γ-H2A.X foci undergo significant changes during the DNA damage response. Initially, a larger number of small foci are formed, while at late stages of the DNA damage response, only a few large foci are usually observed[32]. As expected, large γ-H2A.X foci were formed in control cells starting 4-hours post IR (Figure 4b, *upper panels*) and persisting until 12-hours after IR, while the overall level of γ-H2A.X phosphorylation remains relatively constant. However, this morphological progression was not observed in WSTF RNAi cells despite the initial formation of small γ-H2A.X speckles as in the controls (Figure 4b, *lower panels*). Instead, the amount and intensity of the γ-H2A.X foci were significantly less than in controls (only 16% of the WSTF RNAi retain γ-H2A.X foci 4 hours post IR), and no large foci were observed in WSTF RNAi cells during the entire experiment, even 12 hours post IR (Figure 4b). Since the major kinases for γ-H2A.X phosphorylation are ATM and ATR, and γ-H2A.X foci maintenance is dependent on sustained recruitment of active ATM to the damage foci via Mdc1[17], we asked if the relocalization of ATM and Mdc1 were defective in

WSTF deficient cells. In control cells, large Mdc1 foci were observed at a late stage of the DNA damage response (8-hour post 10 Gy of IR) (Figure 4c), while similar foci were not observed in the WSTF deficient cells, indicating that the recruitment of Mdc1 is defective at a late stage of the DNA damage response in these cells. Autophosphorylation at Ser 1981 (referred to as phos-ATM hereafter) is one of the indicators of ATM activation during the DNA damage response[33],[34],[35]. Foci formation of phos-ATM (and potentially other targets of ATM) was also impaired in WSTF deficient cells (Figure 4d). These data strongly suggest that WSTF plays a critical role in the recruitment of active ATM and Mdc1 to the damage sites, both of which are critical for γ-H2A.X foci formation.

We next investigated if the kinase activity of WSTF is required for its function during the DNA damage response, namely, the maintenance of phos-ATM and γ-H2A.X foci. Since the WSTF mRNA sequences targeted by the short hairpin RNAi constructs are different between human and mouse (see above), we complemented WSTF RNAi cells (derived from mouse 3T3 cells) with WT or C338A mutant kinase domain constructs of human WSTF. This approach successfully restored the expression of kinase domain of WSTF (Figure 4e & f). The expression of the WT WSTF kinase domain rescued the γ-H2A.X and phos-ATM foci formation defects in the WSTF RNAi cells (Figure 4e & f). In nearly 100% of the cells complemented with the WT construct, γ-H2A.X and phos-ATM foci were observed at least 8 hours after DNA damage treatment (Figure 4e & f). On the other hand, the phos-ATM and γ-H2A.X foci formation were as defective in cells expressing the C338A mutant as in WSTF RNAi cells containing vector alone (Figure 4e & f). Taken together, these results demonstrate that WSTF plays an important role during the DNA damage response via its novel kinase activity, an activity that targets H2A.X Y142 and possibly other yet unknown substrates.

We wondered, however, if S139 phosphorylation is required for the steady–state balance of H2A.X phosphorylation at Y142 or vice versa. As previously reported[15],[18], the maintenance of γ-H2A.X phosphorylation is affected in the Mdc1-/- MEF cells (Supplementary Figure S8). Y142, however, becomes gradually dephosphorylated in the Mdc1-/- cells as in the WT control cells (Supplementary Figure S8), indicating that sustained γ-H2A.X phosphorylation is not required for Y142 dephosphorylation. On the other hand, S139 phosphorylation level and foci formation were greatly reduced upon DNA damage in both Y142L and Y142F mutant cells (Supplementary Figure S8). In addition, mutations on Y142 affect Mdc1 binding to H2A.X C-tail phosphorylated at S139 (Supplementary Figure S8). These data suggests that these phosphorylation events may be coordinated during the DNA damage response (see **Discussion** below).

## Discussion

Our studies call attention to a new regulatory mechanism controlling histone H2A.X function mediated by the WSTF-SNF2H (WICH) chromatin remodeling complex. We found a novel phosphorylation site on H2A.X, Y142, and demonstrated that it plays a vital role in the DNA damage response. We also discovered that the amino-terminal domain of WSTF has a previously unrecognized tyrosine kinase activity for this site (see below). WSTF, a gene frequently deleted in the human William Syndrome (WS), has previously been shown

to be the regulatory component of the WICH chromatin remodeling complex[25],[29]. Our findings therefore have identified an unexpected link between a histone minor variant, H2A.X, a histone covalent modification and an ATP-dependent chromatin remodeling mechanisms that control the mammalian DNA damage response.

The kinase domain of WSTF is composed of two putative motifs. The N-motif contains the highly conserved WAC domain, which is found in many eukaryotic proteins, while the C-motif is much more divergent. Besides H2A.X, WSTF may have other downstream targets given its multiple roles in DNA damage repair, replication and transcription. William-Beuren syndrome (WS) is a well-documented genetic disorder characterized by developmental defects and clinical behavioral phenotypes[36], so identifying the link between the biochemical function of WSTF and the clinical manifestation of WS remains a challenge for future studies. In addition, WSTF kinase activity and Y142 phosphorylation may play multiple roles during DDR (see Supplemental Information for a detailed discussion). First, pre-existing phosphorylated Y142 may be needed at the break to adjust local chromatin structure for the later maintenance of S139 phosphorylation. Subsequent dephosphorylation of Y142 after DNA damage could act to enhance Mdc1 and ATM recruitment to extend and maintain γ–H2A.X phosphorylation. Second, WSTF may regulate γ-H2A.X foci maintenance through other pathways and unidentified targets, which may play an important role in recruiting or stabilizing Mdc1 and ATM at damage foci. Finally, in the absence of Y142 phosphorylation, the kinetics of the phosphorylation/dephosphorylation cycle of γ-H2A.X may be altered such that both the phosphorylation and dephosphorylation of H2A.X on S139 occur much more rapidly and the foci form and disassemble in less than 4 hours. Identification of signaling pathways utilizing H2A.X Y142 phosphorylation or other physiologically-relevant phosphorylation events regulated by the WICH chromatin remodeling complex will be of interest in future studies.

## Methods Summary

### Plasmids and cell culture

All plasmid constructs were generated with standard protocols (**Methods**). Recombinant MSCV virus carrying H2A.X or WSTF constructs were packaged in Phoenix cells and used to infect MEFs or NIH 3T3 cells. MSCV virus production and infection followed standard protocols[37]. For each construct, three independent lines were derived. The expression levels were checked by immunoblots and immunofluorescence.

### Purification of H2A.X-containing mononucleosomes and associated protein factors

MEF fractionation and chromatin pellet isolation were performed as described[22]. Chromatin pellets were briefly digested with Mnase (Sigma) and the generation of mononucleosomes was monitored by electrophoresis[38] and subject to MS analysis.

### Generation of recombinant WSTF proteins

Recombinant baculovirus carrying the full length WSTF (Flag-epitope-tagged at C terminus) was produced using the BaculoGold-BEVS Kit (BD Biosciences). The full length WSTF proteins were purified using a published protocol[25]. The viruses that express

truncated WSTF constructs were produced with the Bac-to-Bac (Invitrogen) approach and purified (**Methods**). The N- and C-motif of WSTF kinase domain were generated in *E. coli*. (**Methods**).

### In vitro kinase assay conditions

Recombinant full-length (50ng-100ng) or truncated WSTF proteins (0.1-0.5ug) were incubated with free histone proteins (1-2ug), histone octamers or nucleosomes assembled *in vitro* (500ng-1ug) in 20mM Tris pH 7.4 and 150mM NaCl supplemented with $^{32}$P-γ-ATP (NEN) and 1mM $MnCl_2$, at 25°C for 45 minutes.

## Methods

### Plasmids and cell culture

Tyr142 mutant constructs were derived from WT human H2A.X plasmids (Openbiosystems) using Quickchange kit (Stratagene) and verified by DNA sequencing. Primers: *Y142L forward*: 5′-caagaaggccacccaggcctcccaggagctctaag-3′; *Y142L Reverse*: 5′-cttagagctcctgggaggcctgggtggccttcttg-3′; *Y142F forward*: 5′-caagaaggccacccaggcctcccaggagtt ctaag-3′; *Y142L Reverse: 5′*-cttagaactcctgggaggcctgggtggccttcttg-3′. These plasmids were amplified by PCR and cloned into pTOPO vectors (Invitrogen). Primers: Forward: 5′-cacctcgggccgcggcaagactg-3′ Reverse: WT: 5′-cttagtactcctgggag-3′; Y142L: 5′-cttagagctcctgggag-3′; Y142F: 5′-cttagaactcctgggag-3′.

For generating N-terminal Flag tagged constructs, the WT or mutant H2A.X coding region in the pTOPO vectors were cloned in-frame between the BamH1 and Xho1 sites of the pCMV-Tag2A vectors (Stratagene). Tagged or untagged constructs were cloned into MSCV-puro vectors (gifts from Dr. Herr's lab, University of Zurich, Zurich, Switzerland). To generate constructs for recombinant protein expression in *E. Coli*, the coding regions of the WT or Y142F H2A.X of the untagged vectors (above) were cloned in to pET28 vectors (Novagen), in-frame with the N-terminal 6XHis tag.

MSCV virus production and infection followed standard protocols[37]. In brief, MSCV viruses were packaged in Phoenix cells and used to infect H2A.X -/- MEFs (gifts from Dr. A. Nussenzweig's Lab, NIH, Bethesda, MD), followed by puromycin selection. For each construct, three independent lines were derived. The expression levels of H2A.X were checked by immunoblots and immunofluorescence.

Full-length WSTF (human) constructs was a gift from Dr. Varga-Weisz (Babraham Institute, Cambridge, UK). To generate a series of truncated WSTF constructs for insect cell expression, the PCR fragments of the corresponding regions of the WSTF gene were cloned into a modified pFASTBac vector (Invitrogen), which contains an N-terminal GST and a C-terminal His tag sequence. The C338A mutant (1-359) was derived from the WT 1-359 construct, using the QuickChange site-directed mutagenesis kit (Stratagene) and was verified by DNA sequencing. To generate constructs for protein expression in *E coli*, the PCR product of the N-motif (1-205) was cloned into pGex6p vector (GE Healthcare) in-frame with the N-terminal GST tag, and the PCR product of the C-motif (208-345) was

cloned into a modified pRSFDuet-1 (Novagen) vector in-frame with the N-terminal MBP tag. To generate constructs for mammalian cell expression, the PCR products (the forward primer contains a BamH1 and reverse contains a Xho1 site sequence) of the corresponding fragments of the human WSTF gene were cloned in between the BamH1 and Xho1 sites of pTAG3A vectors (Stratagene), in-frame with the N-terminal Myc epitope tag. The tagged constructs were cloned into MSCV-puro vectors.

### Generation of WSTF RNAi knock-down cells

WSTF RNAi cell lines were generated using recombinant pShag-2 vectors containing shRNA constructs targeting the mouse WSTF gene (Clone ID: V2MM_17087, Openbiosystems). Three independent lines were generated by infecting virus carrying these vectors into NIH3T3 cells and propagated under puromycin. In Figure 4, the WSTF RNAi cells were infected with recombinant MSCV viruses carrying the WT (1-359) or the mutant (C338A) constructs.

### Purification of H2A.X-containing mononucleosomes and associated protein factors

MEF fractionation and chromatin pellet isolation (Figure 2) were performed as described[22]. Chromatin pellets were briefly digested with Mnase (Sigma) and the generation of mononucleosomes was monitored by electrophoresis[38]. 50 μl FLAG-M2 agarose beads were used for immunoprecipitating the total mononucleosomes isolated from $2\times10^8$ cells. The precipitated complex was resolved on 4-12% gradient gels (Invitrogen) and then silver- or coomassie blue stained. The gel bands were isolated and subjected to mass spectrometry.

### Protein Identification by mass spectrometry

Gel-resolved protein were digested with trypsin, batch purified on a reversed-phase micro-tip, and resulting peptide pools individually analyzed by matrix-assisted laser desorption/ ionization reflectron time-of-flight (MALDI-reTOF) mass spectrometry (MS) (*UltraFlex TOF/TOF*; BRUKER; Bremen, Germany) for peptide mass fingerprinting (PMF), as described [39],[40]. Selected peptide ions (*m/z*) were taken to search a “non-redundant” protein database (NR; 3,245,378 entries on 28 January, 2006; National Center for Biotechnology Information; Bethesda, MD) utilizing the PeptideSearch algorithm (Matthias Mann, Max-Planck Institute for Biochemistry, Martinsried, Germany; an updated version of this program was currently available as ‘PepSea’ from Applied Biosystems/MDS Sciex; Foster City, CA). A molecular mass range up to twice the apparent molecular weight (as estimated from electrophoretic relative mobility) was covered, with a mass accuracy restriction of less than 40 ppm, and maximum one missed cleavage site allowed per peptide. To confirm PMF results, mass spectrometric sequencing of selected peptides was done by MALDI-TOF/TOF (MS/MS) analysis on the same prepared samples, using the UltraFlex instrument in ‘LIFT’ mode. Fragment ion spectra were taken to search NR using the MASCOT MS/MS Ion Search program [41], version 2.0.04 for Windows (Matrix Science Ltd., London, UK). Any tentative confirmation of a PMF result thus obtained was verified by comparing the computer-generated fragment ion series of the predicted tryptic peptide with the experimental MS/MS data.

### Immunobloting and immunofluorescence

Cells at 70-80% confluence were exposed to an ionizing radiation source (Cs) to introduce DNA damage (at 10Gy). Samples were collected at indicated time points post irradiation. Histone extraction, cell fractionation, high salt nuclear extraction and western blotting followed standard protocols[42,43]. For immunofluorescence, cells were grown on cover slips and fixed with 3% paraformaldehyde. The subsequent indirect immunofluorescent staining followed standard protocols[43]. For WSTF staining, cells were extracted with a high salt buffer for 2 minutes at 4°C before fixing, as described[28]. Antibodies: γ-H2A.X, α-general H2A.X and α-BRCA1 (Millipore/Upstate); α-WSTF and α-Myc (sigma); α-ATM S1981 phos (Rockland immunological) α-Mdc1, α-BAF53 and α-SNF2H were generous gifts from Dr. Lou (Mayo clinic, MN), Drs. Kim and Roeder (Rockefeller University, NY), and Dr. Reinberg (New York University, NY), respectively.

### Recombinant Mdc1 protein expression and peptide pull-down assay

GST-Mdc1-BRCT protein expression followed manufacturer's protocols (Stratagene). Peptides (UN: N-CPSGGKKATQASQEY-C; S139(ph): N-CPSGGKKATQApSQEY-C; Y142(ph): N-CPSGGKKATQASQEpY-C; S139(ph) &Y142(ph): N-CPSGGKKATQApSQEpY-C; F142: N-CPSGGKKATQASQEF-C; L142: N-CPSGGKKATQASQEL-C S139(ph), L142: N-CPSGGKKATQApSQEL-C; S139(ph), F142: N-CPSGGKKATQApSQEF-C) were conjugated to agarose bead with Sulfolink kit (Pierce). Peptide pull-down experiments were performed as described previously[44].

### Circular dichrowasm measurement

Circular Dichroism (CD) experiments were performed on an Aviv 62A/DS (Aviv Associates, Lakewood, NJ) spectropolarimeter. Spectra (260nm to 200nm) were collected with Cell path length of 0.1cm and bandwidth of 1nm. Samples were diluted to 10uM with 20mM Tris-HCl, pH 7.5, 100mM KCl, 2mM DTT. Protein concentrations were determined with their 280nm absorbance.

### Automated chemical (‘Edman’) protein sequencing

Protein samples were analyzed with a Procise 494 instrument from Applied Biosystems (AB) as described[45]. Stepwise liberated PTH-amino acids were identified using an “on-line” HPLC system (AB) equipped with a PTH C18 (2.1×220 mm; 5 micron particle size) column (AB).

### Mapping WSTF kinase domain and Preparation of recombinant WSTF protein from insect cells

To map the putative kinase domain, we generated a series of protein constructs within the N-terminal regions of WSTF. All these protein constructs were extensively purified (Figure 3a, *right*), and MS analysis did not identify any contaminating protein kinases. The 1-345 construct had much more potent kinase activity (>50 fold) than the 1-340 construct (Figure 3e). Furthermore, the substrate specificity of the 1-345 construct is similar to the full length WSTF (Supplementary Figure S5). These results suggest that the amino acid residues in the surrounding regions of 340-345 are critical for the kinase activity of WSTF. Consistent with

these results, the activity of a point mutant at C338 (C338A) was greatly diminished (<50 fold, Figure 3f). The CD spectrum of this mutant is identical to the WT counterpart (Supplementary Figure S6), indicating this mutation did not alter the global structure of the protein.

Recombinant baculovirus carrying the full length WSTF (Flag-epitope-tagged at C terminus) was produced using the BaculoGold-BEVS Kit (BD Biosciences). The full length WSTF proteins were purified using a published protocol[25]. The viruses that express truncated WSTF constructs were produced with the Bac-to-Bac (Invitrogen) method, all of which were tagged with an N-terminal GST tag and a C-terminal 6XHis tag. Baculoviruses were produced in Sf9 cells, and proteins were expressed in Hi5 suspension cells. For truncated WSTF protein purification, harvested Hi5 cells were suspended in 0.4 M KCl, 20mM Tris, pH 7.5, supplemented with the EDTA-free Complete™ Protease Inhibitor Cocktail tablet (Roche). Whole cell lysates were purified through GSTrap columns (GE Healthcare). After removal of the GST tags by PreScission Protease digestion (GE Healthcare), the protein mixtures were purified by HiTrap SP (GE Healthcare). The recombinant WSTF proteins (peaks form at ∼200mM KCL, 20mM Tris pH 7.5) were further purified with Superdex 75 (GE Healthcare) in the elution buffer (50mM KCl, 20mM Tris, pH 7.5). The monomeric peaks (∼60 KDa) were collected and concentrated for further use. The C338A mutant protein was expressed and purified as the WT protein described above.

### Protein preparation in E. coli

*T*he recombinant plasmid vectors carrying the N- and C-motif constructs (above) were transformed into *E.coli* host strain Rosetta2 (DE3) (Novagen) for protein expression under triple antibiotic selection (ampicillin, kanamycin and chloramphenicol) in LB medium. After overnight induction by 0.4 mM isopropyl β-D-thiogalactoside at 25 °C, cells were harvested in buffer 0.4 M KCl, 20mM Tris, pH 7.5. Co-expressed proteins were affinity purified using Amylose resin (New England Biolabs, MA) against the MBP tag. Maltose-eluted samples were purified through a Superdex 200 column (GE Healthcare) in the elution buffer (50mM KCL, 20mM Tris, pH 7.5). Most proteins were eluted in a single peak that contains GST-tagged WAC N- and MBP-tagged WAC C-motif with a stoichiometry of 1:1.

The N- or C-motif were also expressed separately in Rosetta2 (DE3) (Novagen) cells in parallel. The N-motif was purified with GSTrap column and Superdex 200 (GE Healthcare) and C-motif was purified with Amylose resin (New England Biolabs, MA) and Superdex 200 (GE Healthcare). Most proteins were eluted in a monomeric peak (∼50 KDa).

### Histone protein purification and in vitro assembly of histone octamers and mononucleosomes

Individual free histone proteins (H2A.X, H2B, H3 and H4) were expressed and purified using a standard protocol[46]. N-terminal 6XHis-epitope-tagged WT and F142 H2A.X proteins were purified with Ni Sepharose6 columns (GE Healthcare). The assembly of the histone octamers followed standard protocols[46]. Four recombinant histone proteins were denatured in 8M Guanidine-HCl solutions and dialyzed to 2M NaCl. The crude histone

octamers were further purified through a Superdex 75 column (GE Healthcare). Mononucleosomes were assembled as described[47]. The PCR products of the DNA template (nucleosome positioning sequence (clone 601)[48]) was initially incubated in a reaction buffer[47] supplemented with 2M NaCl and diluted in the same reaction buffer stepwise until the NaCl concentration reached 200mM. The assembly of mononucleosomes was checked by electrophoresis on 5% native PAGE gels.

### In vitro kinase assays

Recombinant full-length (50ng-100ng) or truncated WSTF proteins (0.1-0.5ug) were incubated with free histone proteins (1-2ug), histone octamers or nucleosomes assembled *in vitro* (500ng-1ug) in 20mM Tris pH 7.4 and 150mM NaCl supplemented with $\gamma$-$^{32}$P-ATP (NEN) and 1mM $MnCl_2$ for 45 minutes. In Figure S6, 0.1-1mM of $MnCl_2$ or $MgCl_2$ was supplemented as indicated. The reaction was stopped by adding 2mM EDTA. The reaction mixtures were separated by SDS-PAGE, stained with Coomassie blue and dried. The dried gels were exposed against phosphorimager screens (FujiFilm). The autoradiography images were scanned in phosphorimager (FujiFilm) and analyzed by Image Reader FLA-5000.

## Supplementary Material

Refer to Web version on PubMed Central for supplementary material.

## Acknowledgments

We thank A. Nussenzweig for H2A.X-/- MEF cells, P. Varga-Weisz for WSTF constructs and antibodies, W. Herr for pBABE-puro vectors, J. Kim and R. Roeder for α-BAF53 antibodies, D. Reinberg for α-SNF2H antibodies, Z. Lou for α-Mdc1 antibodies and Mdc1 -/- MEF cells, L. Liang and Q. Li for their assistance in recombinant protein expression and purification, C. H. McDonald and R. G. Cook (Baylor College of Medicine, Protein Chemistry Core Laboratory) and The Rockefeller University Proteomic Core facility for H2A.X peptides. We would like to thank the Millipore antibody development scientists for collaborating with us on the generation of H2A.X Y142 phos antibodies, Cat Number 07-1590. This study was supported by the following sources: Susan G. Komen Breast Cancer Foundation (A.X.), Abby Rockefeller Mauze Trust (H. L. and D. J. P.), The Dewitt Wallace and Maloris Foundations (H. L. and D. J. P.), The Irma T. Hirschl Trust (D.S.), NCI Cancer Center Support Grant P30 CA08748 (L. F. H. E. and P. T), research grants from NIH to S. J. E., S. H. A, and C.D.A, and The Rockefeller University (C. D. A.). S. J. E. is an Investigator with the Howard Hughes Medical Institute. We are grateful to E. Bernstein and E. Duncan for critical reading of the manuscript.

## References

1. Khanna KK, Jackson SP. DNA double-strand breaks: signaling, repair and the cancer connection. Nat Genet. 2001; 27:247–254. [PubMed: 11242102]
2. Zhou BB, Elledge SJ. The DNA damage response: putting checkpoints in perspective. Nature. 2000; 408:433–439. [PubMed: 11100718]
3. Redon C, et al. Histone H2A variants H2AX and H2AZ. Current opinion in genetics & development. 2002; 12:162–169. [PubMed: 11893489]
4. Celeste A, et al. Genomic instability in mice lacking histone H2AX. Science. 2002; 296:922–927. [PubMed: 11934988]
5. Celeste A, et al. H2AX haploinsufficiency modifies genomic stability and tumor susceptibility. Cell. 2003; 114:371–383. [PubMed: 12914701]
6. Reina-San-Martin B, et al. H2AX is required for recombination between immunoglobulin switch regions but not for intra-switch region recombination or somatic hypermutation. J Exp Med. 2003; 197:1767–1778. [PubMed: 12810694]

7. Bassing CH, et al. Histone H2AX: a dosage-dependent suppressor of oncogenic translocations and tumors. Cell. 2003; 114:359–370. [PubMed: 12914700]
8. Unal E, et al. DNA damage response pathway uses histone modification to assemble a double-strand break-specific cohesin domain. Mol Cell. 2004; 16:991–1002. [PubMed: 15610741]
9. Harper JW, Elledge SJ. The DNA damage response: ten years after. Mol Cell. 2007; 28:739–745. [PubMed: 18082599]
10. Morrison AJ, et al. INO80 and gamma-H2AX interaction links ATP-dependent chromatin remodeling to DNA damage repair. Cell. 2004; 119:767–775. [PubMed: 15607974]
11. Downs JA, et al. Binding of chromatin-modifying activities to phosphorylated histone H2A at DNA damage sites. Mol Cell. 2004; 16:979–990. [PubMed: 15610740]
12. van Attikum H, Fritsch O, Hohn B, Gasser SM. Recruitment of the INO80 complex by H2A phosphorylation links ATP-dependent chromatin remodeling with DNA double-strand break repair. Cell. 2004; 119:777–788. [PubMed: 15607975]
13. Park JH, et al. Mammalian SWI/SNF complexes facilitate DNA double-strand break repair by promoting gamma-H2AX induction. EMBO J. 2006; 25:3986–3997. [PubMed: 16932743]
14. Stewart GS, Wang B, Bignell CR, Taylor AM, Elledge SJ. MDC1 is a mediator of the mammalian DNA damage checkpoint. Nature. 2003; 421:961–966. [PubMed: 12607005]
15. Goldberg M, et al. MDC1 is required for the intra-S-phase DNA damage checkpoint. Nature. 2003; 421:952–956. [PubMed: 12607003]
16. Lou Z, Minter-Dykhouse K, Wu X, Chen J. MDC1 is coupled to activated CHK2 in mammalian DNA damage response pathways. Nature. 2003; 421:957–961. [PubMed: 12607004]
17. Stucki M, et al. MDC1 directly binds phosphorylated histone H2AX to regulate cellular responses to DNA double-strand breaks. Cell. 2005; 123:1213–1226. [PubMed: 16377563]
18. Lou Z, et al. MDC1 maintains genomic stability by participating in the amplification of ATM-dependent DNA damage signals. Mol Cell. 2006; 21:187–200. [PubMed: 16427009]
19. Lee MS, Edwards RA, Thede GL, Glover JN. Structure of the BRCT repeat domain of MDC1 and its specificity for the free COOH-terminal end of the gamma-H2AX histone tail. The Journal of biological chemistry. 2005; 280:32053–32056. [PubMed: 16049003]
20. Dimitrov S, Dasso MC, Wolffe AP. Remodeling sperm chromatin in Xenopus laevis egg extracts: the role of core histone phosphorylation and linker histone B4 in chromatin assembly. The Journal of cell biology. 1994; 126:591–601. [PubMed: 8045925]
21. Kleinschmidt JA, Steinbeisser H. DNA-dependent phosphorylation of histone H2A.X during nucleosome assembly in Xenopus laevis oocytes: involvement of protein phosphorylation in nucleosome spacing. EMBO J. 1991; 10:3043–3050. [PubMed: 1915279]
22. Mendez J, Stillman B. Chromatin association of human origin recognition complex, cdc6, and minichromosome maintenance proteins during the cell cycle: assembly of prereplication complexes in late mitosis. Mol Cell Biol. 2000; 20:8602–8612. [PubMed: 11046155]
23. Fyodorov DV, Kadonaga JT. The many faces of chromatin remodeling: SWItching beyond transcription. Cell. 2001; 106:523–525. [PubMed: 11551498]
24. Becker PB, Horz W. ATP-dependent nucleosome remodeling. Annual review of biochemistry. 2002; 71:247–273.
25. Ito T, et al. ACF consists of two subunits, Acf1 and ISWI, that function cooperatively in the ATP-dependent catalysis of chromatin assembly. Genes & development. 1999; 13:1529–1539. [PubMed: 10385622]
26. Poot RA, et al. HuCHRAC, a human ISWI chromatin remodelling complex contains hACF1 and two novel histone-fold proteins. EMBO J. 2000; 19:3377–3387. [PubMed: 10880450]
27. Jones MH, Hamana N, Nezu J, Shimane M. A novel family of bromodomain genes. Genomics. 2000; 63:40–45. [PubMed: 10662543]
28. Poot RA, et al. The Williams syndrome transcription factor interacts with PCNA to target chromatin remodelling by ISWI to replication foci. Nat Cell Biol. 2004; 6:1236–1244. [PubMed: 15543136]
29. Bozhenok L, Wade PA, Varga-Weisz P. WSTF-ISWI chromatin remodeling complex targets heterochromatic replication foci. EMBO J. 2002; 21:2231–2241. [PubMed: 11980720]

30. Kukimoto I, Elderkin S, Grimaldi M, Oelgeschlager T, Varga-Weisz PD. The histone-fold protein complex CHRAC-15/17 enhances nucleosome sliding and assembly mediated by ACF. Mol Cell. 2004; 13:265–277. [PubMed: 14759371]
31. Stopka T, Skoultchi AI. The ISWI ATPase Snf2h is required for early mouse development. Proceedings of the National Academy of Sciences of the United States of America. 2003; 100:14097–14102. [PubMed: 14617767]
32. Dellaire, G.; Bazett-Jones, DP. Cell cycle. Vol. 6. Georgetown, Tex: 2007. Beyond repair foci: subnuclear domains and the cellular response to DNA damage; p. 1864-1872.
33. Bakkenist CJ, Kastan MB. DNA damage activates ATM through intermolecular autophosphorylation and dimer dissociation. Nature. 2003; 421:499–506. [PubMed: 12556884]
34. Lee JH, Paull TT. ATM activation by DNA double-strand breaks through the Mre11-Rad50-Nbs1 complex. Science. 2005; 308:551–554. [PubMed: 15790808]
35. Lee JH, Paull TT. Direct activation of the ATM protein kinase by the Mre11/Rad50/Nbs1 complex. Science. 2004; 304:93–96. [PubMed: 15064416]
36. Francke U. Williams-Beuren syndrome: genes and mechanisms. Human molecular genetics. 1999; 8:1947–1954. [PubMed: 10469848]
37. Fernandez-Capetillo O, et al. H2AX is required for chromatin remodeling and inactivation of sex chromosomes in male mouse meiosis. Dev Cell. 2003; 4:497–508. [PubMed: 12689589]
38. Bellard M, Dretzen G, Giangrande A, Ramain P. Nuclease digestion of transcriptionally active chromatin. Methods Enzymol. 1989; 170:317–346. [PubMed: 2770544]
39. Erdjument-Bromage H, et al. Examination of micro-tip reversed-phase liquid chromatographic extraction of peptide pools for mass spectrometric analysis. J Chromatogr A. 1998; 826:167–181. [PubMed: 9871337]
40. Sebastiaan Winkler G, et al. Isolation and mass spectrometry of transcription factor complexes. Methods. 2002; 26:260–269. [PubMed: 12054882]
41. Perkins DN, Pappin DJ, Creasy DM, Cottrell JS. Probability-based protein identification by searching sequence databases using mass spectrometry data. Electrophoresis. 1999; 20:3551–3567. [PubMed: 10612281]
42. Lennox RW, Cohen LH. Analysis of histone subtypes and their modified forms by polyacrylamide gel electrophoresis. Methods Enzymol. 1989; 170:532–549. [PubMed: 2770549]
43. Sambrook, J.; Russell, DW. Molecular cloning : a laboratory manual. Cold Spring Harbor Laboratory Press; Cold Spring Harbor, N.Y.: 2001.
44. Wysocka J, et al. A PHD finger of NURF couples histone H3 lysine 4 trimethylation with chromatin remodelling. Nature. 2006; 442:86–90. [PubMed: 16728976]
45. Tempst P, Geromanos S, Elicone C, Erdjument-Bromage H. Improvements in microsequencer performance for low picomole sequence analysis. METHODS Companion Meth Enzymol. 1994; 6:248–261.
46. Luger K, Rechsteiner TJ, Richmond TJ. Preparation of nucleosome core particle from recombinant histones. Methods in enzymology. 1999; 304:3–19. [PubMed: 10372352]
47. Steger DJ, Eberharter A, John S, Grant PA, Workman JL. Purified histone acetyltransferase complexes stimulate HIV-1 transcription from preassembled nucleosomal arrays. Proceedings of the National Academy of Sciences of the United States of America. 1998; 95:12924–12929. [PubMed: 9789016]
48. Lowary PT, Widom J. New DNA sequence rules for high affinity binding to histone octamer and sequence-directed nucleosome positioning. Journal of molecular biology. 1998; 276:19–42. [PubMed: 9514715]

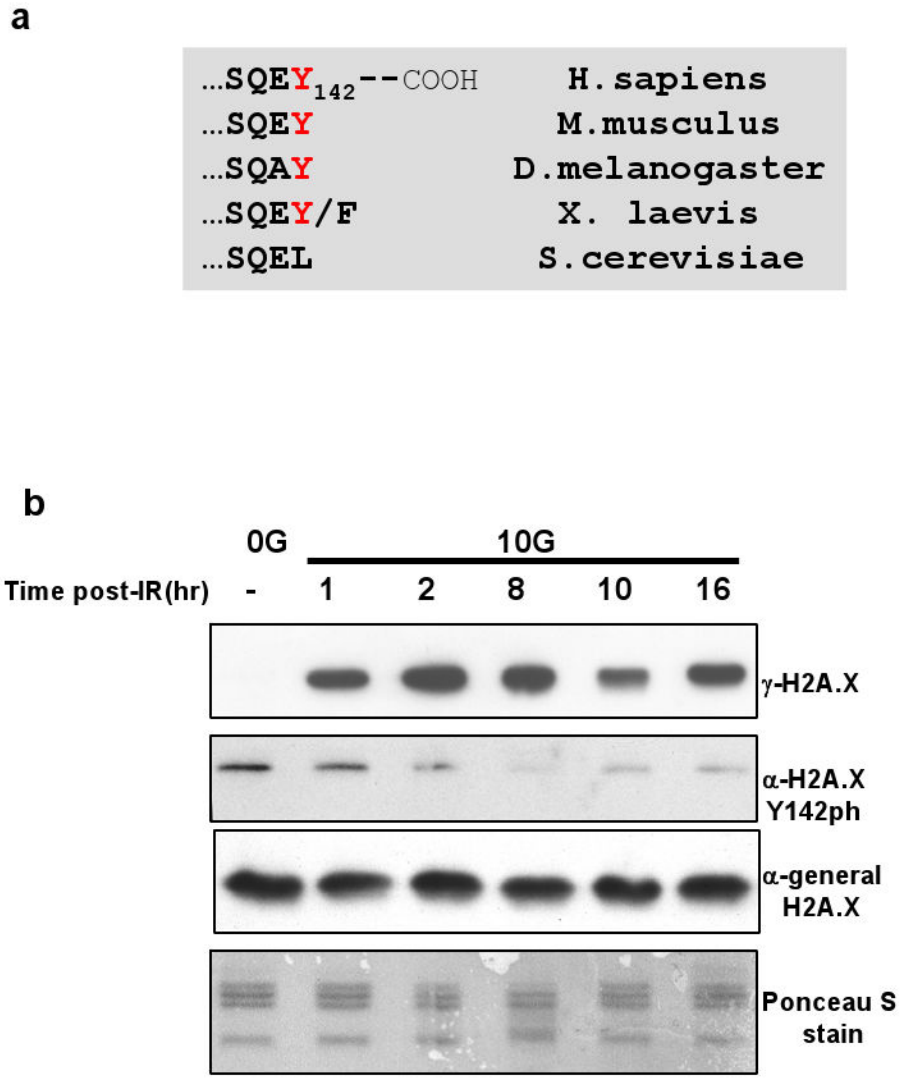


**Figure 1. Y142 of H2A.X is a novel phosphorylation mark regulated by DNA damage signals**

**(a)** Comparison of the extreme C-terminal sequence of H2A.X demonstrates that Tyr142 is conserved in metazoans (mammals, frogs, and fruit flies) but not in unicellular eukaryotes. **(b)** Primary MEF cells were treated with 10 Gy of ionizing radiation (IR) and recovered for a period of time as indicated. Acid-extracted histones were separated by SDS-PAGE and subjected to immunoblotting. H2A.X Y142 phosphorylation levels in MEFs gradually decline, reaching minimum at 8 hr. γ-H2A.X signal is initiated upon damage and maintained up to 16 hours post IR.

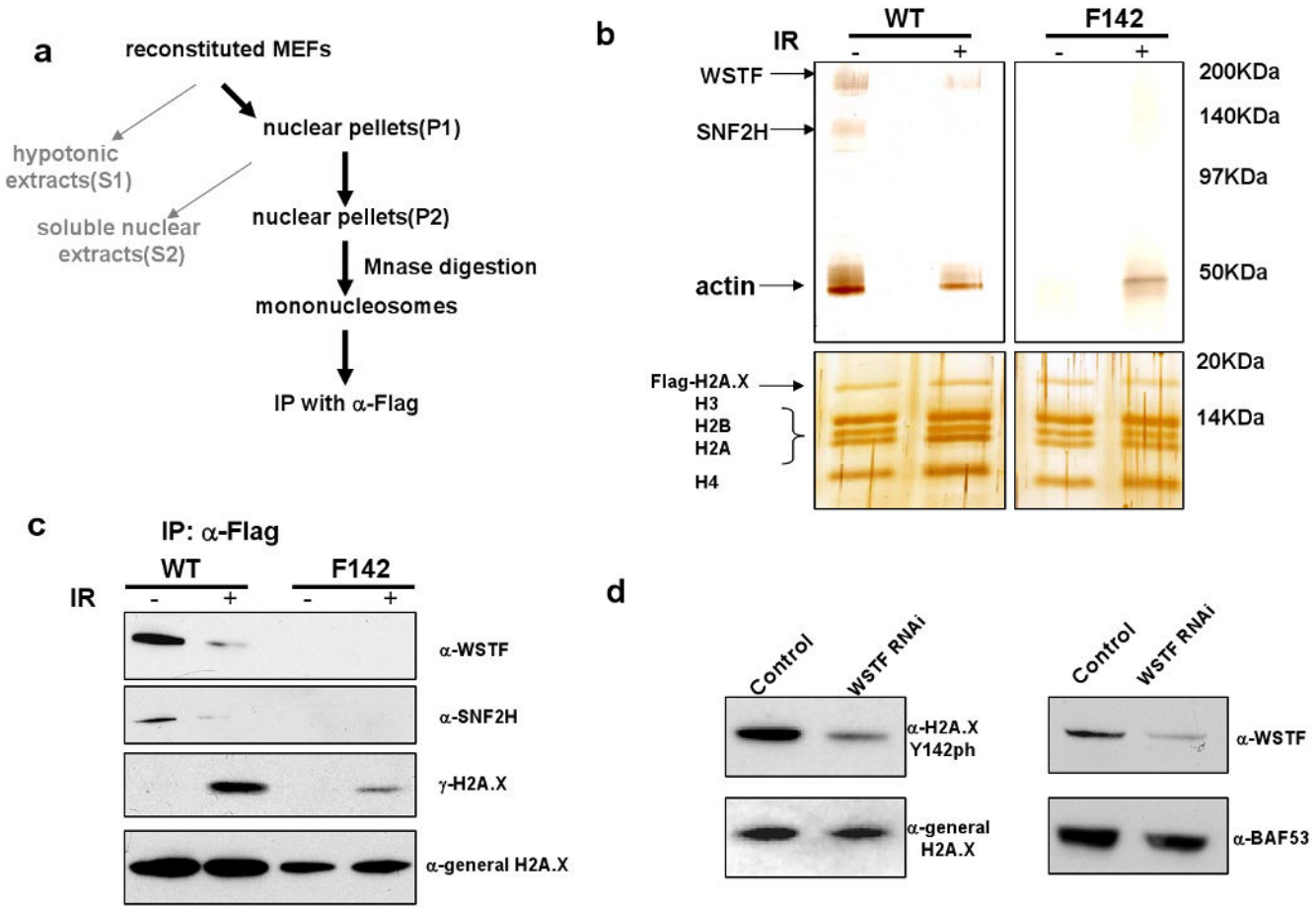


**Figure 2. The WSTF-SNF2H chromatin remodeling complex is specifically associated with H2A.X nucleosomes *in vivo***

**(a)** Purification scheme of H2A.X-containing mononucleosomes. MEFs reconstituted with Flag-H2A.X (WT or Y142F) were treated with or without IR. (**b**) Two polypeptides migrating at 145 and 171 KDa were associated with undamaged WT (*left*), but not the Y142F mutant (*right*) H2A.X-mononucleosomes in a silver-stained gel. Mass spectrometry (MS) analyses revealed these polypeptides as WSTF (171KDa) and SNF2H (145 KDa). The third band at 60 KDa was identified as β–actin in the MS analyses. Staining and MS of the lower molecular weight bands (<20 KDa) revealed similar levels of H2A.X and other core histones. (**c**) The association between the WICH complex and undamaged WT H2A.X mononucleosomes was confirmed by IP-western experiments. (**d**) In WSTF RNAi cells, the expression level of WSTF was significantly diminished; and H2A.X Y142 phosphorylation level was significantly reduced.

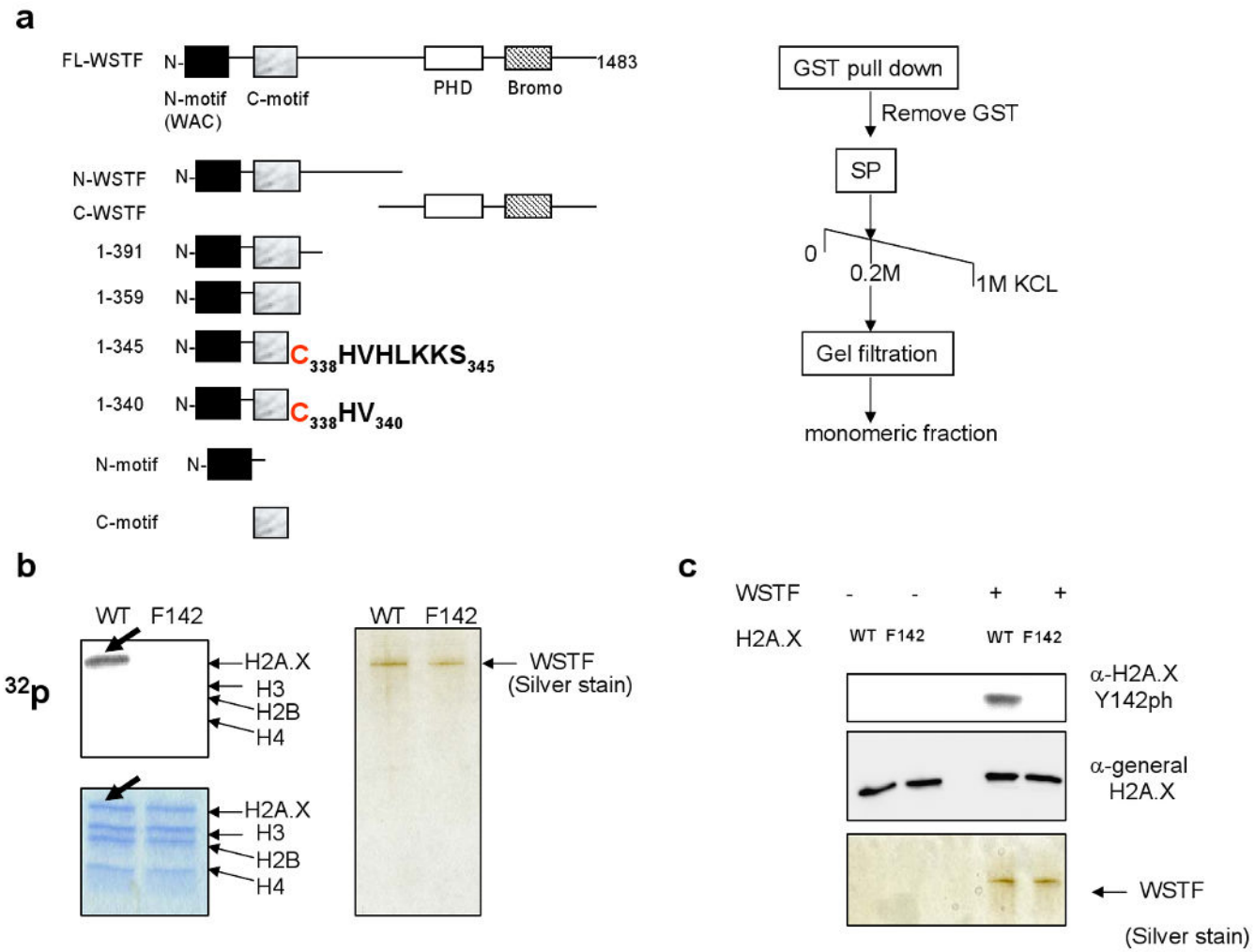

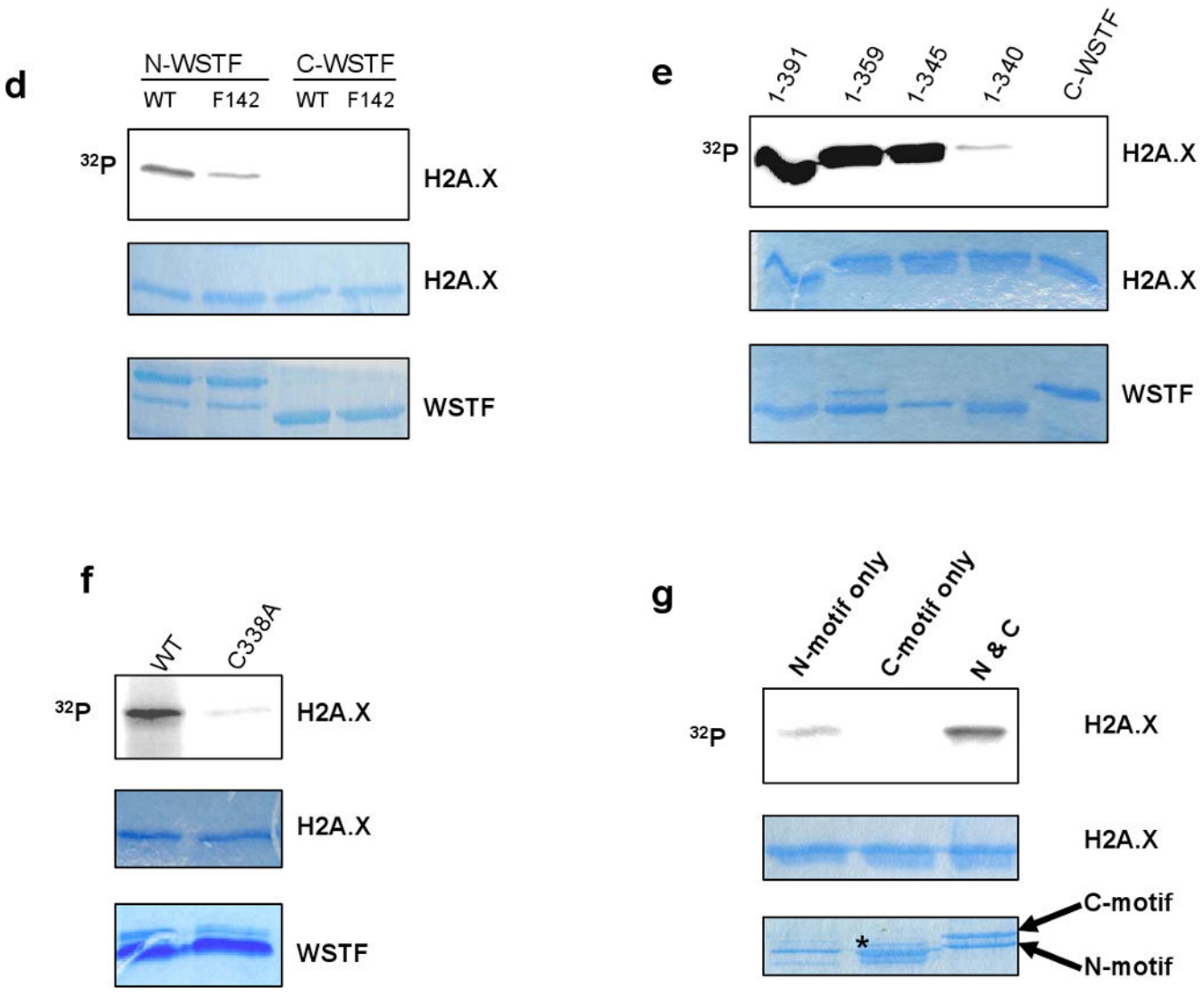


**Figure 3. WSTF contains a novel kinase domain that phosphorylates Y142 of H2A.X**

**(a)** Schematic demonstration of the domain architecture of the human WSTF protein and a series of recombinant proteins representing portions of WSTF. **(b)-(f)** recombinant WSTF proteins were generated in insect cells; and the N- and C- motifs (**g**) were generated in *E. Coli*. **(b)** Y142 in the nucleosome is phosphorylated by recombinant full length WSTF protein. **(c)** The specific phosphorylation of H2A.X at Y142 was detected by immunoblotting with Y142ph antibodies. In **(d)-(g),** free H2A.X proteins were used as substrates in *in vitro* kinase assays. **(d)** N-WSTF, but not C-WSTF, had kinase activity. **(e)** The WSTF 1-340 construct had much reduced kinase activity (<50 fold) in comparison to the other constructs. (**f**) The C338A point mutant (derived from WT 1-359) had much reduced kinase activity. This mutation does not change the global folding properties of the kinase domain (Supplementary Figure S6). (**g**) The co-expressed N-motif and C-motif had significant kinase activity towards H2A.X, while the N-motif alone had a minimal kinase activity. Note: The C-motif construct, when expressed alone, was unstable and partially

degraded from its C-terminus, however, it was protected when co-expressed with the N-motif.

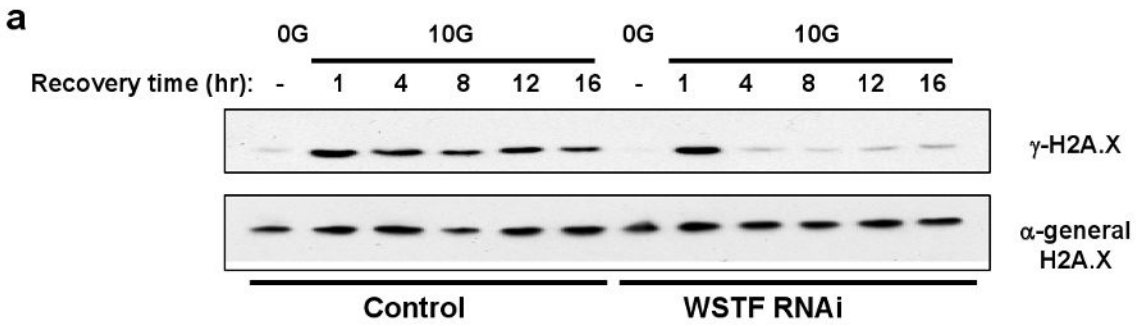


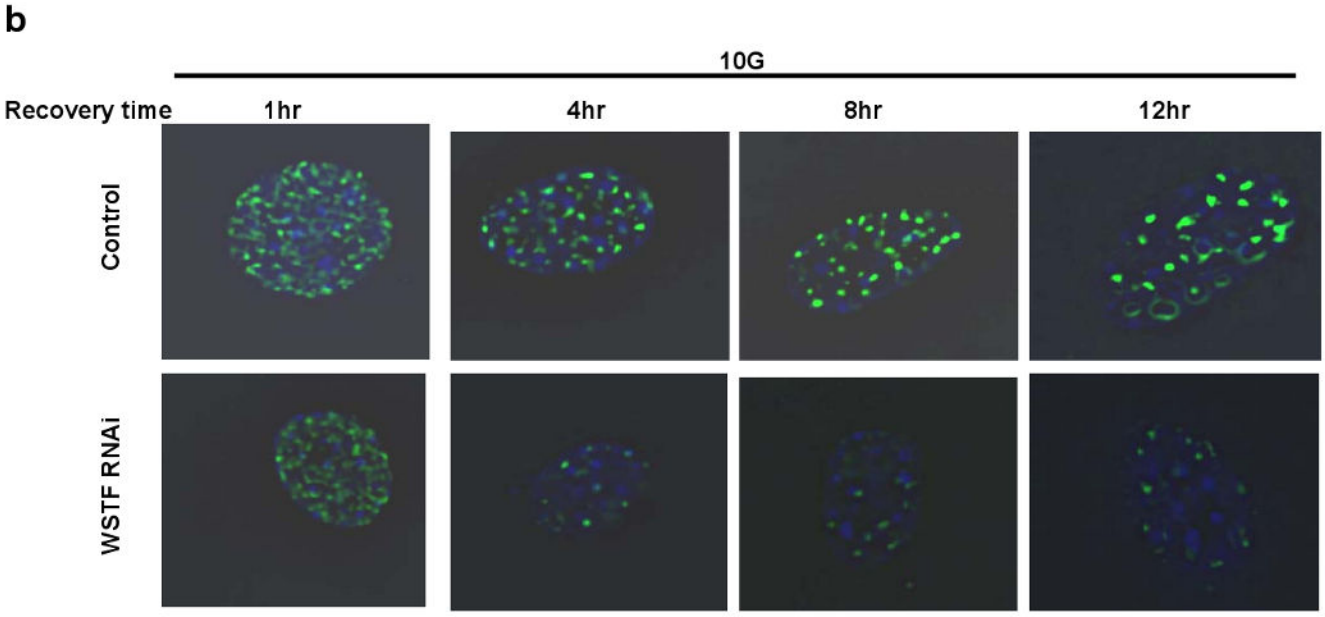


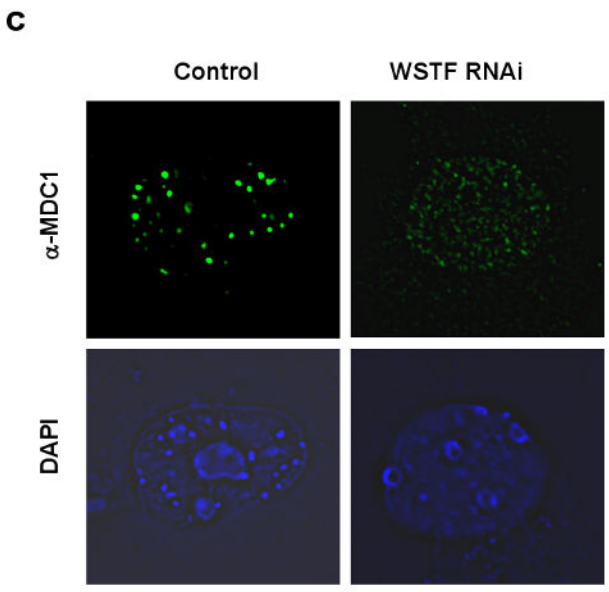


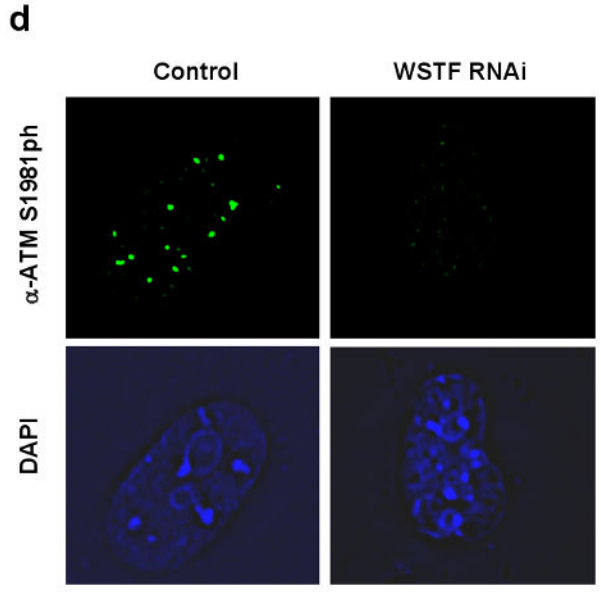

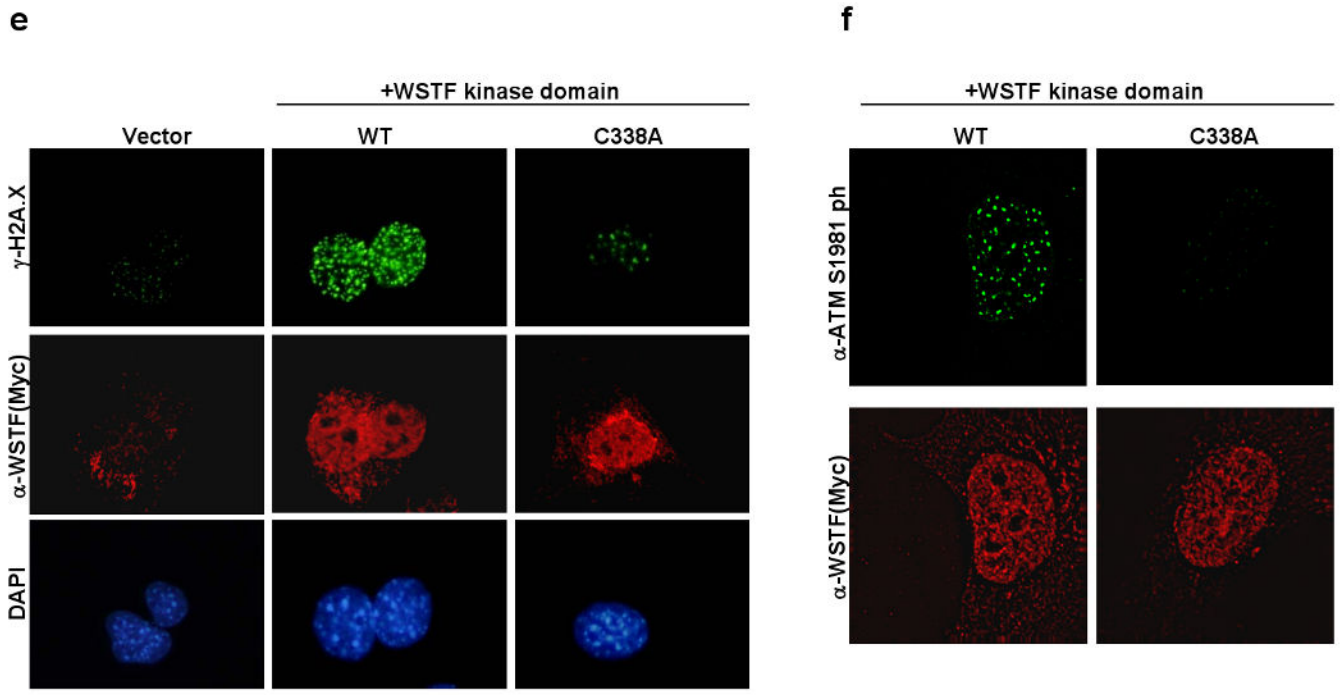


**Figure 4. WSTF is critical for the maintenance of γ-H2A.X phosphorylation after DNA damage**

(**a**) γ-H2A.X maintenance is defective in WSTF RNAi cells after DNA damage treatment. The time points labeled indicate the recovery time following the IR treatment. (**b**) Immunofluorescent staining experiments were performed on control and WSTF RNAi cells fixed at different time points (as labeled) following 10 Gy of IR treatment. (**c & d**) Mdc1 and phos-ATM recruitment are also defective in WSTF deficient cells. Immunofluorescent staining experiments were performed with α-ATM S1981 phos and α-Mdc1 antibodies on control or WSTF RNAi cells, 8-hour post 10 Gy of IR treatment. (**e**) WSTF RNAi cells were complemented with the WT or mutant (C338A) kinase domain constructs (1-359, Myc epitope-tagged at N-terminus) of WSTF. Eight hours after treated with 10 Gy of IR, cells were fixed and co-stained with γ-H2A.X (green) and α-myc antibodies (red). (**f**) The kinase activity of WSTF (red) is also critical for phos-ATM foci maintenance (green).